

Three-Color FRET expands the ability to quantify the interactions of several proteins involved in actin filament nucleation

Horst Wallrabe^{1,2*}, Yuansheng Sun¹, Xiaolan Fang², Ammasi Periasamy^{1,2} and George Bloom²

¹ Keck Center for Cellular Imaging; ² Department of Biology,
University of Virginia, Charlottesville, VA.

* Contact: hw5m@virginia.edu

ABSTRACT

With traditional 2-color Förster Resonance Energy Transfer (FRET) microscopy, valuable quantitative analyses can be conducted. Correlations of donor (D), acceptor (A) and their ratios (D:A) with energy transfer efficiency (E%) or distance (r) allows measurement of changes between control and experimental samples; also, clustered vs. random assembly of cellular components can be differentiated. Essentially, only the above three parameters D, A and D:A vs. E% are the basis for these deductions. 3-color FRET uses the same basic parameters, but exponentially expands the opportunities to quantify interrelationships among 3 cellular components. We investigated a number of questions based on the results of a triple combination (F1-F2-F3) of TFP-NWASP/Venus-IQGAP1/mCherry-Actin – all involved in the nucleation of actin - to apply the extensive analysis assay possible with 3-color FRET. How do changing N-WASP or IQGAP1 fluorescence levels affect actin fluorescence? What is the effect on E% of NWASP-actin by IQGAP1 or E% of IQGAP1-actin by N-WASP? These and other questions are explored in the context of all proteins of interest being in FRET distance vs. any two in the absence of the third. 4 cases are compared based on bleed-through corrected FRET: (1) all 3 interact, (2) only F1-F3 and F2-F3 [not F1-F2], (3) only F1-F2 and F2-F3 interact [not F1-F3], (4) only F1-F2 and F1-F3 interact [not F2-F3]. Other than describing the methodology in detail, several biologically relevant results are presented showing how E% (i.e. distance), fluorescence levels and ratios are affected in each of the cases. These correlations can only be observed in a 3-fluorophore combination. 3-color FRET will greatly expand the investigative range of quantitative analysis for the life-science researcher.

Key words: Three-color FRET, IQGAP1, N-WASP, actin, E%, quantitative analysis, Teal, Venus, mCherry

1. INTRODUCTION

Actin nucleation resulting in actin filaments provide mechanical support for cells as part of the cytoskeleton; they participate in many cellular motility activities, such as in morphogenesis, actin branch formation driving lamellipodial and filopodial extensions, a network for cellular cargo motors, as well as pathogenic processes such as cancer and microbial invasion – to name a few. The process of producing filamentous actin (F-actin) from monomers is dynamic, highly regulated and involves an astounding number of protein effectors, depending on the signals and cues that drive the demand for specific actin nucleation targets¹. Playing such an important role in cellular function, actin nucleation has been experimentally investigated for its many roles with biochemical in-vitro assays, in-vitro TIRF microscopy tracking nucleation and branch formations^{2,3} fluorescence microscopy either in antibody-stained fixed cells and GFP-type fusion proteins in live cells. The data presented here investigates the roles of N-WASP, an activator of the Arp23 complex, which is known to be active at the leading edge of cells where it forms new daughter branches off an existing mother filament and IQGAP1, a scaffold protein⁴. IQGAP1⁵ is an ~380 kDa homodimeric protein⁶ that is widely expressed among vertebrate cell types from early embryogenesis^{7,8} through adulthood^{6,9}. Several sequentially arranged functional domains enable IQGAP1 to bind directly to a rich spectrum of cytoskeletal, adhesion and regulatory proteins^{3,10},

including F-actin (Bashour et al., 1997; Fukata et al., 1997). Its wide role has been reviewed in some excellent papers^{1,11-13}.

Förster (or fluorescence) resonance energy transfer (FRET) is an excellent technique to monitor not only protein-protein interactions¹⁴ but also the organization of proteins at the nanometer level in intracellular membranes, cytosol and other substrates¹⁵. The monitoring of protein-protein interactions in vivo or in vitro and the accuracy of FRET measurement using microscopy techniques has tremendously increased after the introduction of various mutant forms of green fluorescent proteins (GFPs)¹⁶⁻¹⁸. Energy transfer efficiency (E%) represents a powerful tool to investigate and quantify the interactions of effectors of the nucleation of actin and other biological processes involving protein-protein interactions and co-localizations. FRET is the non-radiative transfer of excited-state energy from one molecule (the donor) to another nearby molecule (the acceptor), via a long-range dipole-dipole coupling mechanism¹⁹. For energy transfer to take place, four conditions have to be met. First, there has to be significant overlap between the donor fluorophore emission spectra and the acceptor fluorophore excitation spectra. Second, the average distance between donor and acceptor fluorophore molecules should be around 1 to 10 nm. Third, there has to be optimal dipole-dipole orientation of donor and acceptor molecules. Fourth, the donor has to exhibit sufficient quantum yield. Since energy transfer itself is a dipole-dipole interaction, no photons are transferred. Certain issues of FRET microscopy need to be addressed when attempting quantitative approaches. Because of the spectral overlap, necessary for FRET to occur in the first place, the signal also contains donor crosstalk and acceptor bleed-through. The overlap between the donor and acceptor emission spectra results in donor crosstalk. Acceptor bleed-through occurs when the donor excitation wavelength excites part of the absorption spectrum of the acceptor. Emission filters with different bandwidths have been used to remove donor crosstalk and acceptor bleed-through contamination, provided this does not cause a major reduction in the FRET signal. Different algorithm-based correction methodologies exist and have been reviewed previously²⁰. We have developed a highly sensitive algorithm, based on single label reference specimens, which corrects the contaminated FRET signal in a pixel-by-pixel manner (processed FRET=PFRET algorithm)²¹. Energy transfer efficiency (E%) is the prime parameter for judging the level of relative molecular distances and the robustness of interaction, higher E% being equivalent to closer associations between two fluorophores.

3-color FRET potential correlations	E% and Distance (r)			Fluorophores			Fluorophore Ratios		
	F1-F2	F1-F3	F2-F3	F1	F2	F3	F1:F2	F1:F3	F2:F3
F1 Fluorescence	★	★	★	★	★	★	☆	☆	★
F2 Fluorescence	★	★	★	★	★	★	☆	☆	★
F3 Fluorescence	★	★	★	★	★	★	☆	☆	★
F1:F2 Ratio	★	★	★	☆	☆	★	★	★	★
F1:F3 Ratio	★	★	★	☆	☆	★	★	★	★
F2:F3 Ratio	★	★	★	☆	☆	★	★	★	★

Figure 1. Three-color FRET optional correlations compared with 2-color FRET (dotted line region). Filled stars indicate most relevant correlations, open stars are potentially circular.

Two-color FRET has made considerable progress in quantitative analysis, going beyond just proving interaction between two cellular components of interest. However, when for example multiple proteins interact such as in the nucleation of actin, several double-label experiments have to be conducted to draw some conclusions about the interaction or otherwise between any pair. Even then, we have no information about the impact of one protein on the others within an identical temporal and spatial context. This need led to the development of an algorithm for 3-color FRET²², which obviates the use of double-label specimens and exponentially increases the quantitative analysis potential between 3 proteins. Figure 1 lists all possible correlations and parameters. The solid stars represent most viable analysis targets, open stars indicate potential circularity; some are the inverse of another. Nevertheless a large selection is available to pursue relevant biological questions in a quantitative manner.

All of the preconditions of 2-color FRET have to be met by 3-color FRET. On the face of it, this may limit the number of suitable fluorophores, but in practice, there are sufficient candidates available. We chose TFP-Venus-mCherry. The 3-color combination meets the spectral overlap conditions on paper as well as in practice (Figure 2). The data presented here not only demonstrates the utility of this quantitative assay, but allows us to ask additional questions about how rising levels of one protein or the ratio or distance of two proteins effect the third one. There are challenges inherent in live-cell microscopy and the ability for cells to express 3 fusion proteins, the large number of proteins involved in actin nucleation, while only being able to track 3 labeled components at a time and their usually short-lived interactions.

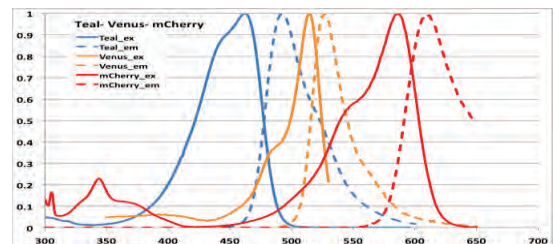


Figure 2. Teal-Venus-mCherry excitation and emission spectra

Nevertheless, important information was obtained demonstrating the value of 3-color FRET and the still growing legacy of Theodor Förster's contribution to FRET microscopy.

2. MATERIAL and METHODS

2.1 Plasmid construction/mutagenesis

The pVenus-hIQGAP1 was constructed by replacing the mGFP cDNA in previously constructed pmGFP-C1-hIQGAP1 with Venus cDNA. The pmGFP-C1-hIQGAP1 (digested by AgeI and XhoI) and Venus cDNA (PCR products digested by AgeI and XhoI) were ligated using T4 DNA ligase by NEB (catalog # M0202S). Venus cDNA was amplified by PCR using pVenus-C1 as template and following primers were used (5' primer: 5'-TTTACCGGTCGCCACCATGGTGAGCAAGGGC-3', 3' primer: 5'-CGTCGACTGCAGAATTCGAAGCTTGAGCTCGAG-3'). Five colonies were analyzed by restriction digestion and cell transfection, and all appeared to be successful, and were further confirmed by sequencing. The correct candidate plasmids were further amplified using HiSpeed Plasmid Maxi Kit by Qiagen (Catalog #12663).

The TFP-hNWASp was constructed using restriction digestion and ligation. The pYFP-C1 vector (digested by NdeI and EcoRI), TFP cDNA (digested from pmTFPC1rC-EBPa by NdeI, BsrGI) and hNWASp (PCR products digested by BsrGI and EcoRI) were ligated using T4 DNA ligase by NEB (catalog # M0202S). pmTFPC1rC-EBPa was kindly provided by Dr. Richard Day. hNWASp cDNA was amplified by PCR from pBluescriptR-hWASL clone by OpenBiosystems (Clone ID #5264663) and following primers were used (5' primer: 5'-AAAAAAAAA TGTACAAG TCCGGA ATGAGCTCCGTCCAGCAGCA-3', 3' primer: 5'-CCG GAATTC TCAGTCTTCCCCTCATC-3'). Eight colonies were analyzed by restriction digestion and all appeared to be successful, and were further confirmed by sequencing. The correct candidate plasmids were further amplified using HiSpeed Plasmid Maxi Kit by Qiagen (Catalog #12663).

The mCherry-actin plasmid was a kind gift from Dr. Derek A. Applewhite, Northwestern University, Chicago, IL 60611

2.2 Cell Cultures & transfections

MDCK cells were grown to ~70-80% confluency, trypsinized with Triple-X (Gibco), re-suspended with growth media (Gibco DMEM+10% Cosmic Calf Serum (CCS) +1% gentamycin) and plated in 2ml aliquots at 1×10^6 density on 25mm sterile cover slips in 6-well dishes. In the meantime, DNA plasmids were incubating with Lipofectamine 2000 (Invitrogen) as per manufacturer's protocol and were added drop-wise immediately after cell plating to their respective cover slips. Single-label cover slips received 4 μ g of DNA of TFP-N-WASP, Venus-IQGAP1, mCherry-Actin. Triple-label cover slips received a total of 4 μ g of DNA, Venus-IQGAP1 in each case 2 μ g and the two other each 1 μ g; these concentrations were based on previously gained experience to test expression efficiencies. Transfected cells were grown for 24 hours and imaged.

2.3 Three-color Confocal FRET Microscopy

Confocal FRET imaging was carried out on a Leica TCS SP5 X confocal / spectral microscope system²³. The system is controlled by the Leica LAS AF software (www.leicamicrosystems.com). Images were acquired using a 60X / 1.2NA water-immersion objective lens on a temperature-controlled stage for the live-cell specimens. The Leica system carries several laser modules: the Argon 458 nm laser line (Ex1) was used as the excitation source for mTFP; the Argon 514 nm laser line (Ex2) was used to excite Venus; mCherry was excited at 581 nm (Ex3) selected from the white light laser (WLL) module, which is tunable from 470 ~ 670 nm in 1-nm increments. Laser power was controlled through acousto-optical tunable filters (AOTF) and optimized for each excitation wavelength. Three emission channels were set up using acousto-optical beamsplitter (AOBS) and three identical photomultiplier tubes (PMT): 468 ~ 515 nm (Em1) for mTFP; 525 ~ 585 nm (Em2) for Venus; 595 ~ 750 nm (Em3) for mCherry. All three PMTs used the same confocal pinhole and were applied with the same configurations i.e. gain and offset. Combining the excitation wavelengths and the emission channels results in 6-channel imaging required for 3-color FRET – Ex1/Em1, Ex1/Em2, Ex1/Em3, Ex2/Em2, Ex2/Em3 and Ex3/Em3. Acquired images were processed and analyzed using the proprietary PFRET algorithm²² to generate PFRET and E% (E in percentage) images.

3. RESULTS and DISCUSSION

3.1 Proof-of-principle with 2-color FRET

Before proceeding to 3-color FRET, we tested for suitability the different fluorophore combinations with 2-color FRET experiments and also established that each of the 3 pairs, N-WASP/IQGAP1, N-WASP-actin and IQGAP1-actin showed FRET interactions, fully corrected for background and spectral bleed-through using our PFRET software^{21,24} (Data not shown). We furthermore tested that the interactions were largely non-random. The standard assay for this condition to be met is the independence of E% on the Acceptor^{15,25,26}. While there is usually an element of randomness, the data demonstrates that the interactions are indeed non-random by virtue of a large data set with a sufficiently wide range of acceptor values (data not shown).

3.2 Triple fluorophore combination Teal-N-WASP/Venus-IQGAP1/mCherry-actin – Four possible interactions

While there are additional effectors involved in the nucleation of actin, we have studied several triple combinations from the proteins shown in Figure 3; we report here on a subset for the combination of Teal-N-WASP/Venus-IQGAP1/mCherry-Actin, which are symbolized in Figure 4 as Fluorophore 1 (F1), Fluorophore 2 (F2) and Fluorophore 3 (F3). There are four FRET interactions possible (Figure 5) and the data was analyzed separately for these four categories and compared: In case #1, all 3 fluorophores show fully corrected FRET interactions, with F2 and F3 being both acceptors to F1, and F2 being simultaneously donor to F3. In Case #2, N-WASP and IQGAP1 interact with actin without FRET between N-WASP and IQGAP1 (F1-F2). In Case #3, IQGAP1 interacts with N-WASP and actin, but there is no FRET between N-WASP-actin (F1-F3). In Case #4, N-WASP interacts with IQGAP1 and actin, but there is no FRET between IQGAP1 and actin (F2-F3).

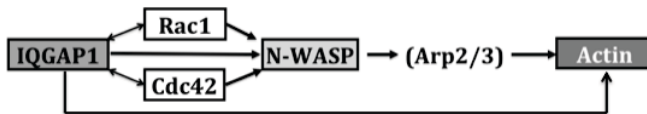


Figure 3. Interacting proteins of interest in the nucleation of actin. Shaded IQGAP1, N-WASP and actin are the focus of this report.

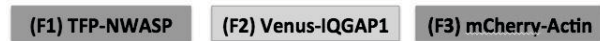


Figure 4. The three fusion proteins involved in this 3-color quantitative FRET experiment

Having determined the specific FRET interrelationships, we proceeded to separate the data into these four potential cases for analysis. The determination of which parameters and correlations listed in Figure 1 are most applicable to this triple combination are based on what is known from biochemical *in vitro* data and published results generally. We have chosen to compare the four cases with respect to (a) average fluorescence of each protein, (b) average E% (and the related relative distance) between the three pairs, (c) all data points of actin fluorescence as a function of either IQGAP1 or N-WASP, (d) all data points of E% between N-WASP-actin as a function of IQGAP1 and E% IQGAP1-actin as a function of N-WASP, (e) All data points for the ratio of N-WASP: actin as a function of IQGAP1 and the ratio of IQGAP1-actin as a function of N-WASP. In addition to showing the usual trend-line for the total data set, correlation coefficients by small accumulating bins on the x-axis are also charted for two reasons: effectors in the complex process of actin nucleation are known to effect their regulation by subtle changes in their concentration – expressed here in fluorescence levels; second, potential overexpression of fusion proteins may be inferred when a correlation threshold or plateau is reached, made visible by accumulated bins.

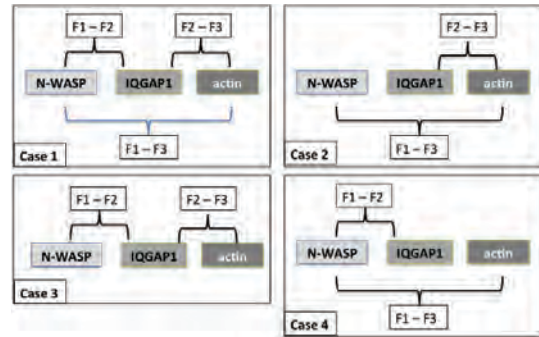


Figure 5. FRET interactions can occur 4 different ways. Case 1: all interact; Case 2: all, but N-WASP-IQGAP1; Case 3: all, but N-WASP-actin; Case 4: all, but IQGAP1-actin

The images were processed and analyzed with the PFRET software with four different thresholds to isolate these four cases as per Table 1. The thresholds for non-interaction were set at $\leq 5\%$ PFRET and $\leq 5\%$ E%, having to meet only one of these parameters to be classified thus. Surprisingly, Case 3 had most regions of interest (ROIs) with 4508 where IQGAP1 interacts with both, N-WASP and actin, but N-WASP does not do so with actin. When all three proteins FRET in Case1, 1825 data point arise. Cases 2 and 4 (224 and 163 ROIs respectively) have only a fraction of cases 1 and 3 ROIs, providing initial evidence that IQGAP1 needs to interact with both, N-WASP and actin simultaneously as in cases 1 and 3. Figure 6 represents an example of images used for data analysis; this set also reflects the overall differences in populations between the four cases, case 3 having the largest number of ROIs.

Interactions by case based on PFRET/E% (Thresholds)				
	Case 1	Case 2	Case 3	Case 4
# of data points	1825	222	4508	163
F1 - F2 (NW-IQ1)	YES (>5%)	NO (<5%)	YES (>5%)	YES (>5%)
F1 - F3 (NW-actin)	YES (>5%)	YES (>5%)	NO (<5%)	YES (>5%)
F2 - F3 (IQ1-actin)	YES (>5%)	YES (>5%)	YES (>5%)	NO (<5%)

Table 1. Parameters for segmenting data into 4 cases. Non-FRET was determined to be PFRET <5 and/or E% <5%, any one threshold being sufficient

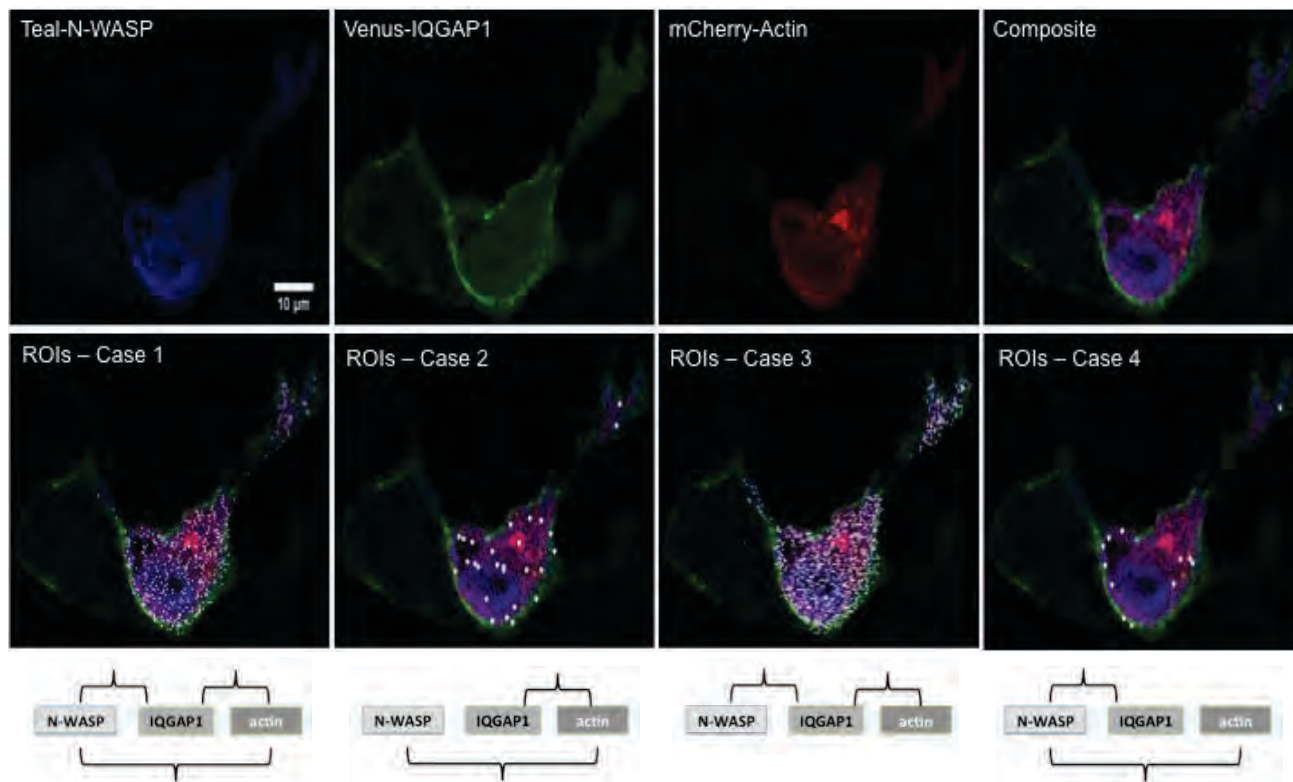


Figure 6. An example of images used for quantitative analysis. The Teal-N-WASP image is based on Teal excitation/Teal emission, the other two are analogously Venus excitation/Venus emission and mCherry excitation/mCherry emission. The composite image is used on the ROIs by case 1-4, representing the overall situation of Case 3 having most ROIs, followed by Case 1.

2.3 Average fluorescence and E% data as a first step to compare 4 cases

Average fluorescence (Figure 7) is statistically different between cases by ANOVA (Table 2), bearing in mind the very much lower populations in cases 2 and 4. Comparing E% (Figure 8), being an expression of relative distance, case 3 stands out as exhibiting highest E% (closest distance) between NWASP-IQGAP1 and IQGAP1/Actin, when there is no interaction between NWASP and Actin.

Averages, supported by ANOVA statistics provide useful information about the 4 data sets, such as a sufficient level of labeled proteins to ensure that biological functionality is likely, even if they are statistically different.

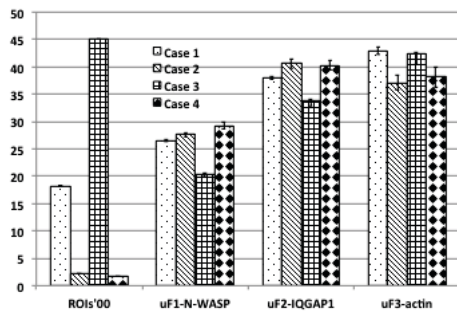


Figure 7. Mean fluorescence of N-WASP, IQGAP1 and actin, comparing cases 1-4. The number of ROIs (x100) are for information.

ANOVA - Analysis of Variance (One-Way)					
N-WASP	Case 1	Case 2	Case 3	Case 4	p-value
Mean	26.52	27.57	20.46	29.23	0.E+0
IQGAP1					
Mean	38.02	40.58	33.78	40.3	0.E+0
Actin					
Mean	42.94	37.1	42.29	38.13	0.004

ANOVA - Analysis of Variance (One-Way)					
E% N-WASP-IQGAP1	Case 1	Case 2	Case 3	Case 4	p-value
Mean	25.71	3.00	46.25	18.6	0.E+0
E% N-WASP-actin					
Mean	20.34	27.87	0.67	25.16	0.E+0
E% IQGAP1-actin					
Mean	29.56	25.39	39.29	3.37	0.E+0

Table 2 (top) and Table 3 (bottom) both show that populations in Cases 1-4 are statistically different

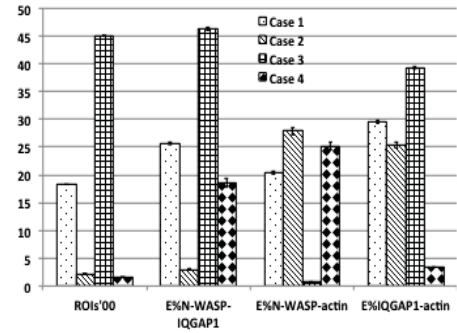


Figure 8. Mean E% comparing cases 1-4, equivalent to distances between fluorophores. Higher E% = closer distance

3.4 Actin fluorescence as a function of IQGAP1 or N-WASP – comparing 4 cases

As mentioned in the introduction, even beyond the proteins shown in Figure 3, there are other endogenous effectors of actin nucleation at work in this live-cell assay. Here, we are recording quantitatively the behavior of the three labeled proteins N-WASP, IQGAP1 and actin. Figures 9 and 10 are looking at actin fluorescence as correlated to accumulating levels of IQGAP1 or N-WASP, each in the presence of the other, comparing the 4 cases to ascertain, whether the one or other non-interaction has an impact on actin. As shown in Table 3, while ANOVA p-value for actin for the 4 cases results in a statistical difference, when IQGAP1 interacts with both, N-WASP and actin (Cases 1 & 3), the average

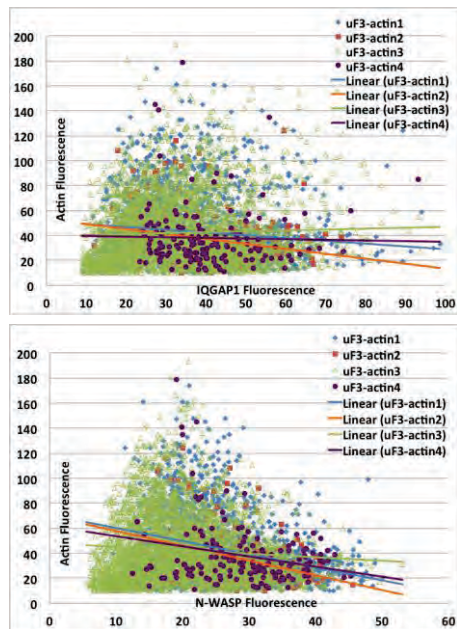


Figure 9. All data points by case of actin as a function of IQGAP1 (top) or N-WASP (bottom). Trend lines are refined in Fig. 10

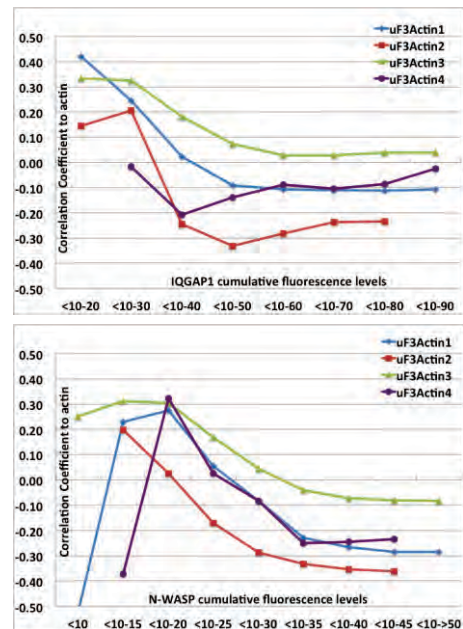
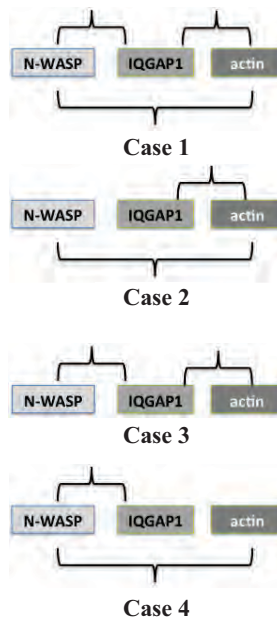


Figure 10. Correlation coefficients vs. actin by accumulated fluorescence steps of IQGAP1 (top) and N-WASP (bottom)

fluorescence of actin is identical; it is also higher than in Cases 2 and 4. The correlation coefficients by the step-wise accumulation of IQGAP1 and N_WASP is different between these two vs. actin. Both reflect *in vitro* results (not shown) that most significant changes occur at lower concentrations, here related to levels of fluorescence. IQGAP1 reaches a plateau at ~ 50 gray-level units, when further increases show actin's independence of IQGAP1. N-WASP starts at a negative, changing to a positive correlation, only to decline into negative territory – Case 1 being the 'base-case' when all interact. The most negative correlation occurs in Case 2, when IQGAP1 and N-WASP do not 'FRET', confirming the importance of IQGAP1 as a scaffold protein and regulator of actin nucleation^{2,27}.

3.5 E% IQGAP1-actin vs. N-WASP and E% N-WASP-Actin vs. IQGAP1 – comparing 4 cases

Energy transfer efficiency (E%) being an expression of distance may provide an insight about the relative association/binding dynamics between two proteins in this assay as a function of the third in the four cases under reference. For information, E% data points are shown for IQGAP-Actin in case 4, where no interaction has been determined, (Figure 11/top); correlation coefficients by cumulative N-WASP, however, for case 4 are not meaningful and are not included (Figure 12/top). The same applies to E% N-WASP-actin for Case 3 (Figures 11 & 12/bottom). Tables 2 and 3 and Figure 8 already established the average E%s between proteins, Cases 1 and 3 resulting in largest E%s between IQGAP1-actin. Viewing this as a function of cumulative increases of N-WASP, the correlation is becoming increasingly negative in Cases 1 and 3, while in Case 2 the decline is similar, starting however at high correlation coefficient levels.

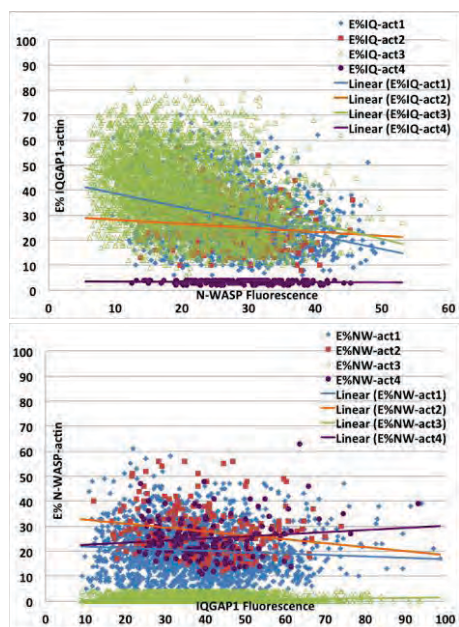


Figure 11. All data points by case of E% IQGAP1-actin vs. N-WASP (top) or E% N-WASP-actin vs. IQGAP1 (bottom). Trend lines are refined in Fig. 12

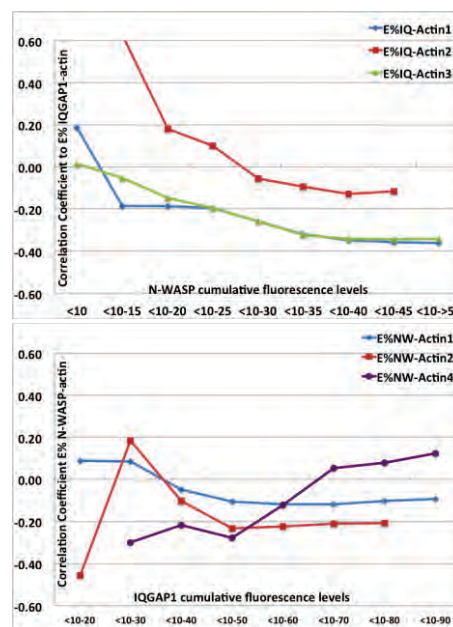
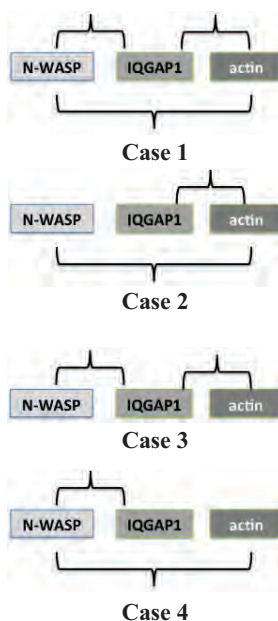


Figure 12. Correlation coefficient of E% IQGAP1-actin by accumulating N-WASP (top) or E% N-WASP-actin by accumulating IQGAP1 (bottom).

3.6 IQGAP1: actin Ratio vs. N-WASP and N-WASP: actin Ratio vs. IQGAP1 – comparing 4 cases

Another way of looking at the data is to explore whether the ratio of IQGAP1: actin is affected by N-WASP or whether the opposite is true where the ratio of N-WASP: actin is affected by IQGAP1, or whether both affect each other, respectively, which would provide clues about putative regulatory functions. Figure 13 shows again all data points for above two correlations. In this case data for the IQGAP: actin ratio for Case 4 (no FRET between the two) is excluded for being non-meaningful. The same applies to the N-WASP: actin ratio for Case 3. Comparing the overall correlations

in Figure 13 (top), rising N-WASP drives the IQGAP1: actin ratio with more IQGAP1 associating with actin. The more refined, stepwise correlation shows differences in correlation coefficients at low N-WASP fluorescence

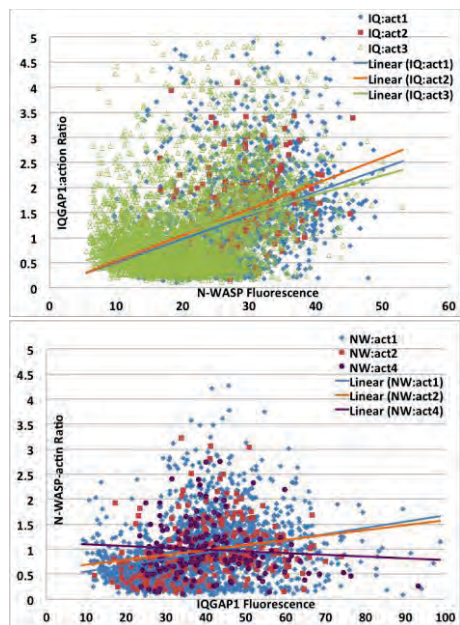


Figure 13. All data points by case (except Case 4 - not meaningful) of the IQGAP1: actin ratio vs. N-WASP (top) or N-WASP: actin vs. IQGAP1 (bottom), except Case 3 – not meaningful.

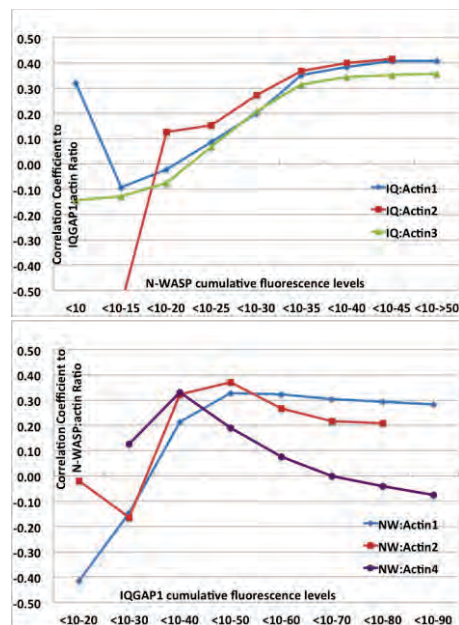


Figure 14. Correlation coefficient of IQGAP1: actin ratio by accumulating N-WASP (top) or N-WASP: actin ratio by accumulating IQGAP1 (bottom).

(‘concentration’), particularly in Case 2, where N-WASP and IQGAP1 do not FRET. IQGAP1’s effect on the N-WASP: actin ratio again sees the most significant changes at lower fluorescence levels, however, instead of increasing the amount of N-WASP associating with actin, rising IQGAP1 levels either reach a threshold or the correlation becomes non-dependent (Case 4).

While separating the live-cell FRET data into 4 cases provides a potential window into the interrelationships of the three labeled proteins, it has to be kept in mind that numerous other endogenous effectors are participating in the signaling cascade, which regulates actin nucleation. Nevertheless, we may assume that these are present in all four cases. Another consideration are the rapid kinetics of interaction; the surprisingly largest data occurs in Case 3 (4508 ROIs), when IQGAP1 interacts with both, N-WASP and actin, but N-WASP does not FRET with actin. This may indicate the slowest kinetic association, followed by Case 1 (when all interact, 1825 ROIs) at the instant of confocal microscopy image acquisition of live cells. The much smaller number of data points for Case 2 (222 ROIs) and Case 4 (163 ROIs) may just be stages pre- or post-cycling off by the non-interacting protein.

The 3-color FRET assay opens up new possibilities to investigate 3 spatially and temporally interacting components, allowing an unprecedented level of analysis and correlations.

ACKNOWLEDGEMENTS

This work was supported by NIH grant NS051746.

REFERENCES

- 1 Chhabra, E. S. & Higgs, H. N. The many faces of actin: matching assembly factors with cellular structures. *Nat Cell Biol* **9**, 1110-1121, doi:10.1038/ncb1007-1110 (2007).
- 2 Benseñor, L. B. *et al.* IQGAP1 regulates cell motility by linking growth factor signaling to actin assembly. *J Cell Sci* **120**, 658-669 (2007).
- 3 Mateer, S. C. & Bloom, G. S. IQGAPs: integrators of the cytoskeleton, cell adhesion machinery and signaling networks. *Cell Motil. Cytoskel.* **55**, 147-155 (2003).
- 4 Padrick, S. B. & Rosen, M. K. Physical mechanisms of signal integration by WASP family proteins. *Annu Rev Biochem* **79**, 707-735, doi:10.1146/annurev.biochem.77.060407.135452 (2010).
- 5 Weissbach, L. *et al.* Identification of a human rasGAP-related protein containing calmodulin-binding domains. *J. Biol. Chem.* **269**, 20517-20521 (1994).
- 6 Bashour, A.-M., Fullerton, A. T., Hart, M. J. & Bloom, G. S. IQGAP1, a Rac- and Cdc42-binding protein, directly binds and cross-links microfilaments. *Journal of Cell Biology* **137**, 1555-1566 (1997).
- 7 Cupit, L. D., Schmidt, V. A., Miller, F. & Bahou, W. F. Distinct PAR/IQGAP expression patterns during murine development: implications for thrombin-associated cytoskeletal reorganization. *Mamm Genome* **15**, 618-629 (2004).
- 8 Yamashiro, S., Noguchi, T. & Mabuchi, I. Localization of two IQGAPs in cultured cells and early embryos of *Xenopus laevis*. *Cell Motil Cytoskeleton* **55**, 36-50, doi:10.1002/cm.10109 (2003).
- 9 Takemoto, H. *et al.* Localization of IQGAP1 is inversely correlated with intercellular adhesion mediated by e-cadherin in gastric cancers. *Int J Cancer* **91**, 783-788 (2001).
- 10 Briggs, M. W. & Sacks, D. B. IQGAP proteins are integral components of cytoskeletal regulation. *EMBO Rep.* **4**, 571-574 (2003).
- 11 Brandt, D. T. & Grosse, R. Get to grips: steering local actin dynamics with IQGAPs. *EMBO Rep* **8**, 1019-1023, doi:10.1038/sj.embor.7401089 (2007).
- 12 Gao, C. *et al.* IQGAP1 regulates NR2A signaling, spine density, and cognitive processes. *J Neurosci* **31**, 8533-8542, doi:10.1523/JNEUROSCI.1300-11.2011 (2011).
- 13 Kim, H., White, C. D. & Sacks, D. B. IQGAP1 in microbial pathogenesis: Targeting the actin cytoskeleton. *FEBS Lett* **585**, 723-729, doi:10.1016/j.febslet.2011.01.041 (2011).
- 14 Wallrabe, H. & Periasamy, A. Imaging protein molecules using FRET and FLIM microscopy. *Curr Opin Biotechnol* **16**, 19-27, doi:10.1016/j.copbio.2004.12.002 (2005).
- 15 Wallrabe, H., Elangovan, M., Burchard, A., Periasamy, A. & Barroso, M. Confocal FRET microscopy to measure clustering of ligand-receptor complexes in endocytic membranes. *Biophys J* **85**, 559-571, doi:10.1016/S0006-3495(03)74500-7 (2003).
- 16 Dobbie, I. M., Lowndes, N. F. & Sullivan, K. F. Autofluorescent proteins. *Methods Cell Biol* **85**, 1-22, doi:10.1016/S0091-679X(08)85001-7 (2008).
- 17 Giepmans, B. N., Adams, S. R., Ellisman, M. H. & Tsien, R. Y. The fluorescent toolbox for assessing protein location and function. *Science* **312**, 217-224, doi:10.1126/science.1124618 (2006).
- 18 Tsien, R. Y. & Miyawaki, A. Seeing the machinery of live cells. *Science* **280**, 1954-1955 (1998).
- 19 Periasamy, A., Wallrabe, H., Chen, Y. & Barroso, M. Chapter 22: Quantitation of protein-protein interactions: confocal FRET microscopy. *Methods Cell Biol* **89**, 569-598, doi:10.1016/S0091-679X(08)00622-5 (2008).
- 20 Berney, C. & Danuser, G. FRET or no FRET: a quantitative comparison. *Biophys J* **84**, 3992-4010, doi:10.1016/S0006-3495(03)75126-1 (2003).
- 21 Elangovan, M. *et al.* Characterization of one- and two-photon excitation fluorescence resonance energy transfer microscopy. *Methods* **29**, 58-73 (2003).
- 22 Sun, Y., Wallrabe, H., Booker, C. F., Day, R. N. & Periasamy, A. Three-color spectral FRET microscopy localizes three interacting proteins in living cells. *Biophys J* **99**, 1274-1283, doi:10.1016/j.bpj.2010.06.004 (2010).
- 23 Sun, Y. *et al.* Characterization of an orange acceptor fluorescent protein for sensitized spectral fluorescence resonance energy transfer microscopy using a white-light laser. *J Biomed Opt* **14**, 054009, doi:10.1117/1.3227036 (2009).
- 24 Chen, Y. & Periasamy, A. Intensity range based quantitative FRET data analysis to localize protein molecules in live cell nuclei. *J Fluoresc* **16**, 95-104, doi:10.1007/s10895-005-0024-1 (2006).

- 25 Kenworthy, A. K., Petranova, N. & Edidin, M. High-resolution FRET microscopy of cholera toxin B-subunit and GPI-anchored proteins in cell plasma membranes. *Mol Biol Cell* **11**, 1645-1655 (2000).
- 26 Wallrabe, H., Bonamy, G., Periasamy, A. & Barroso, M. Receptor complexes cotransported via polarized endocytic pathways form clusters with distinct organizations. *Mol Biol Cell* **18**, 2226-2243, doi:10.1091/mbc.E06-08-0700 (2007).
- 27 Le Clainche, C. *et al.* IQGAP1 stimulates actin assembly through the N-WASP-Arp2/3 pathway. *J Biol Chem* **282**, 426-435, doi:M607711200 [pii]10.1074/jbc.M607711200 (2007).